

# Raman measurements on thin films of the $\text{La}_{0.7}\text{Sr}_{0.3}\text{MnO}_3$ manganite: a probe of substrate-induced effects

P. Dore<sup>1,a</sup>, P. Postorino<sup>1</sup>, A. Sacchetti<sup>1</sup>, M. Baldini<sup>1</sup>, R. Giambelluca<sup>1</sup>, M. Angeloni<sup>2</sup>, and G. Balestrino<sup>2</sup>

<sup>1</sup> Coherentia CNR-INFM and Dipartimento di Fisica, Università “La Sapienza”, P.le A. Moro 4, 00187 Roma, Italy

<sup>2</sup> Coherentia CNR-INFM and Dipartimento di Ingegneria Meccanica, Università di Roma Tor Vergata, via del Politecnico 1, 00133 Roma, Italy

Received 27 July 2005

Published online 16 December 2005 – © EDP Sciences, Società Italiana di Fisica, Springer-Verlag 2005

**Abstract.** We report on a Raman study of the phonon spectrum of  $\text{La}_{0.7}\text{Sr}_{0.3}\text{MnO}_3$  thin films epitaxially grown on  $\text{LaAlO}_3$ . The spectrum, as a function of film thickness  $d$ , does not change over the 1000–100 Å range, whereas a strong hardening of the phonon frequencies of both bending and stretching modes is apparent in ultra-thin films ( $d < 100$  Å) where substrate-induced effects are remarkable. This behaviour, which appears to be related with the measured  $d$ -dependence of the insulator-to-metal transition temperature, is ascribed to co-operative effects of  $\text{MnO}_6$  octahedra rotation and charge-localization. Raman spectroscopy proves to be a simple and powerful tool to monitor subtle structural modifications hardly detectable with conventional diffraction techniques in ultra-thin films.

**PACS.** 63.20.-e Phonons in crystal lattices – 78.20.-e Optical properties of bulk materials and thin films – 78.30.-j Infrared and Raman spectra

## 1 Introduction

It well known that several pseudocubic manganites like  $\text{La}_{1-x}\text{Ca}_x\text{MnO}_3$  and  $\text{La}_{1-x}\text{Sr}_x\text{MnO}_3$  with  $0.2 < x < 0.5$  show colossal magnetoresistance (CMR) around the insulator-to-metal transition which occurs at a characteristic temperature  $T_P$  close to the Curie temperature  $T_C$  [1,2]. A complete understanding of these phenomena has not yet been achieved, although the key role of the lattice degrees of freedom, besides the double-exchange interaction basically responsible for electrical transport below  $T_P$ , is widely recognised. Indeed magnetotransport properties strongly depend on the extent of the electron-phonon coupling triggered by Jahn-Teller (JT) distortions of the oxygen octahedra around the  $\text{Mn}^{3+}$  ions [3].

Thin manganite films, essential for possible technological applications, have been the subject of intense investigation focused on both growth methods and characterisation [4]. The role of the film-substrate lattice mismatch on the structural and transport properties has been in particular investigated. It is generally recognised that thick films show bulk-like structure and properties, whereas substrate-induced effects become important when making the film thinner. It has been observed that the value of  $T_P$  starts decreasing as the film thickness  $d$  gets smaller than a critical value  $d_c$  and finally vanishes when  $d < d_0$ . How-

ever the values of  $d_c$  and  $d_0$  as reported in the literature are spread over a wide range even when dealing with the same film/substrate system [5,6]. Different mechanisms, such as epitaxial strain [7,8], finite size effect [9,10], and the occurrence of a dead-layer at the film/substrate interface [11,12] have been proposed to explain the  $d$ -dependence of  $T_P$ .

Raman spectroscopy is an ideal tool for investigating these systems since the vibrational modes of the  $\text{MnO}_6$  octahedra, which are crucial in determining transport properties of manganites, contribute with the most intense peaks of the Raman-active phonon spectrum. A number of papers dealing with bulk and thick film samples witnesses the relevance and sensibility of this technique [13]. In the present work we exploit Raman spectroscopy to study the  $d$ -dependence of the phonon spectrum of  $\text{La}_{0.7}\text{Sr}_{0.3}\text{MnO}_3$  (LSMO) films and to demonstrate its capability in probing substrate-induced effects in thin films.

## 2 Experiment

Films having a carefully controlled cation and oxygen stoichiometry were grown by pulsed laser deposition on different substrates [14]. Raman spectra were measured in back-scattering geometry, using a micro-Raman spectrometer equipped with a CCD detector and a notch filter to reject the elastic contribution. The sample was excited by the

<sup>a</sup> e-mail: paolo.dore@roma1.infn.it

632.8 nm line of a He-Ne Laser. The confocal microscope was equipped with a 50 X objective, which allows obtaining a laser spot about  $5 \mu\text{m}^2$  wide at the sample surface. Spectra have been collected within the  $200\text{--}1100 \text{ cm}^{-1}$  frequency range with a spectral resolution of about  $3 \text{ cm}^{-1}$ . A very small confocal diaphragm ( $50 \mu\text{m}$ ) was used to limit the scattering volume, thus reducing the signal due to the substrate as much as possible.

Preliminary measurements have been carried out on LSMO films grown on different substrates, namely  $\text{NdGaO}_3$  (001),  $\text{SrTiO}_3$  (110), and  $\text{LaAlO}_3$  (001), to test the feasibility of an accurate Raman analysis. Among these substrates the best choice is  $\text{LaAlO}_3$  (LAO) because of its low-intensity and simply structured Raman signal, given by a dominant sharp peak at  $485 \text{ cm}^{-1}$  within the spectral range of interest [15]. Therefore, Raman measurements on LSMO/LAO films allowed us to extract the phonon spectrum of LSMO even for very thin films, down to  $40 \text{ \AA}$ , when the substrate largely affects the measured signal. For these films, sample characterisation has shown a fully relaxed structure for thickness above  $d_c \cong 160 \text{ \AA}$ , and a disruption of the transport properties for thickness below  $d_0 \cong 80 \text{ \AA}$ , ascribed to the existence of a dead-layer at the film/substrate interface [14].

To study the  $d$ -dependence of the LSMO phonon spectrum we measured several LSMO/LAO films in the  $1000\text{--}40 \text{ \AA}$   $d$  range. An acquisition time ranging from 30 min (thicker films) to 90 min (thinner films) was enough to obtain low-noise Raman spectra.

### 3 Results and discussion

Raman spectra of LSMO/LAO films for four representative  $d$  values (800, 320, 160, and  $80 \text{ \AA}$ ), and the spectrum of one of the thinnest measured films ( $40 \text{ \AA}$ ) are shown in Figures 1a and 1b, respectively. On decreasing  $d$ , although the Raman signal arising from the substrate progressively increases, the overall spectral shape due to LSMO film basically does not change and closely resembles that obtained for bulk samples of different CMR manganites [15–18]. The spectrum mainly consists of three broad components around  $300$ ,  $500$ , and  $620 \text{ cm}^{-1}$  usually ascribed to rotational (R), bending (B), and stretching (S) modes of the  $\text{MnO}_6$  octahedron, respectively [16, 19]. In agreement with previous reports [15, 20], a weak peak around  $430 \text{ cm}^{-1}$  (component X) is also detectable (see Fig. 1). In some of the measured spectra (e.g. the  $160$  and  $40 \text{ \AA}$  films in Fig. 1a) an unexpected extra component (E) around  $730 \text{ cm}^{-1}$  is clearly visible. Its origin is unclear and we have not been able to find out an unambiguous correlation between the growth conditions and its presence and/or its intensity. In any case, by directly comparing the Raman spectra obtained in films nominally grown in the same conditions, with or without the E component, we clearly observed that this component is an additional contribution with no appreciable influence on the other spectral components.

We have applied a fitting procedure in order to distinguish and analyze the contribution due to the manganite

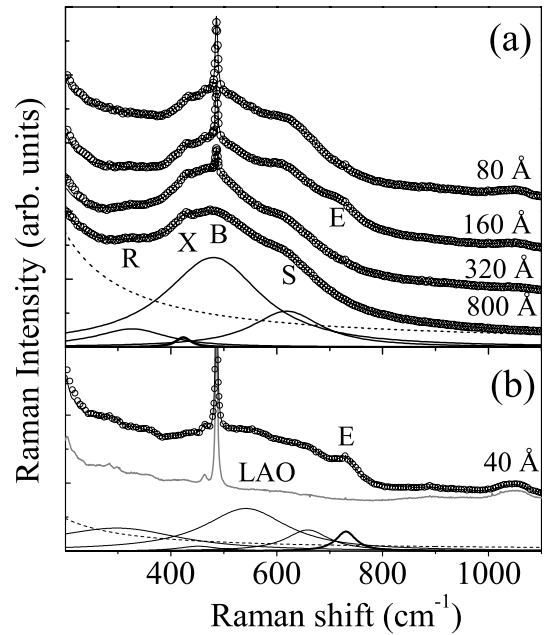


**Fig. 1.** Raman spectra (open symbols) and best fit profiles (full lines) of the 80, 160, 320, 800 (panel a) and  $40 \text{ \AA}$  (panel b) films. In (a), the four components (R, X, B, and S) of the  $800 \text{ \AA}$  film are indicated and the corresponding best fit profiles are shown separately, as well as the electronic background (dashed line). In (b), the best fit components and the LAO contribution (grey line) are shown separately. In the  $160$  and  $40 \text{ \AA}$  spectra the observed E component is indicated.

film and to quantitatively determine the  $d$ -dependence of the different Raman components. We assumed the measured spectra  $S(\nu)$  to be given by the sum of two contributions arising from the LSMO film and the LAO substrate, i.e.  $S(\nu) = S_{\text{LSMO}}(\nu) + F S_{\text{LAO}}(\nu)$ . We used the measured Raman spectrum of LAO ( $S_{\text{LAO}}(\nu)$ ) multiplied by the adjustable normalizing factor  $F$ , and a standard model function, given by the linear combination of damped harmonic oscillators plus an electronic term [19, 20], for  $S_{\text{LSMO}}(\nu)$ . The above assumption, although reasonable, is furthermore justified a posteriori by the quite good agreement between the experimental data and the fitting function, as shown in Figure 1. The  $S_{\text{LSMO}}(\nu)$  term, i.e. the model spectrum of the manganite film, properly accounts for all the spectral features discussed above, i.e. the R, X, B, S, and E (when observed) components. The most interesting results have been obtained for the thickness-dependence of the peak frequencies of the bending ( $\nu_B$ ) and stretching ( $\nu_S$ ) phonons (see Fig. 2a). The error bars on the  $\nu_B$  and  $\nu_S$  values reported in Figure 2a are representative of both the uncertainty of the best-fit parameter values and the slight differences between best-fit values obtained for different films with the same nominal thickness. We would like to stress that films having the same thickness do not show any appreciable difference (within the experimental error) in the  $\nu_B$  and  $\nu_S$  values regardless the E component. Figure 2a shows a large and rather abrupt increase of  $\nu_B$  and  $\nu_S$  on decreasing  $d$  in ultra-thin films

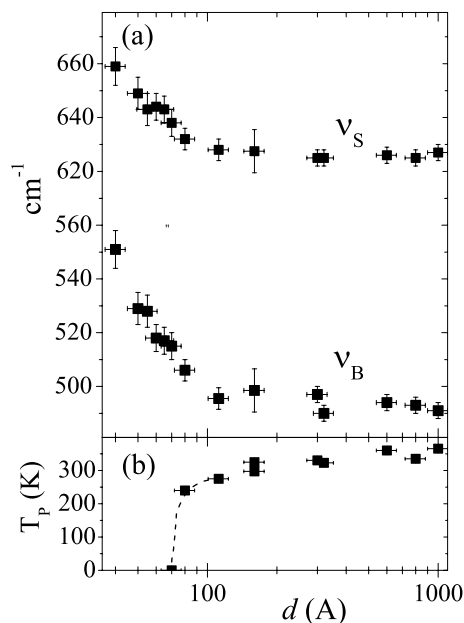


**Fig. 2.** Peak frequency of the bending ( $\nu_B$ ) and stretching ( $\nu_S$ ) phonons (panel a) and transition temperature  $T_P$  (panel b) as a function of the film thickness  $d$ . The dashed line in (b) is just a guide to the eye, indicating that films below 80 Å do not show a metallic phase.

( $d < 100$  Å). This behavior, to be ascribed to a remarkable substrate-induced structural effect, appears to be related to the measured  $d$ -dependence of  $T_P$  which is shown in Figure 2b.

The observed continuous evolution of the phonon spectrum on decreasing  $d$  suggests a continuous evolution of the film structure, although the small- $d$  behaviour of  $\nu_B$  and  $\nu_S$  shows up the onset of some kind of a progressive structural rearrangement involving  $\text{MnO}_6$  octahedra at around  $d = 100$  Å. In particular, since the bending mode appear to be the most sensitive to  $d$ , a rotation of the octahedra towards new equilibrium positions matching more and more closely the in-plane substrate structure is suggested. On the other hand, also the rather abrupt disappearance of the metallic phase, as shown in Figure 2b, leads to similar conclusions. Indeed the large extent of charge-localization, which prevents metallization in ultra-thin film, can be associated to large distortion of the octahedra which, therefore, can be allocated in the pseudocubic lattice only by varying the tilt angle Mn-O-Mn among them. The above interpretation of the Raman results is supported by recent synchrotron X-ray experiments [10, 22]. Indeed, the analysis of an angular resolved absorption study on a LSMO/LAO thin film ( $d = 450$  Å) does not show modification of the tilt angle [10], whereas diffraction data on thin and ultra-thin  $\text{La}_{0.7}\text{Ca}_{0.3}\text{MnO}_3$  films grown on  $\text{SrTiO}_3$  substrate ( $24 < d < 800$  Å), clearly show a reorientation of the  $\text{MnO}_6$  octahedra for the 24 Å thick film [22].

Within the above framework, the dead-layer, which appears to be responsible [14] of the full disruption of the

film transport properties (Fig. 2b), consists of a distorted manganite layer where a structural rearrangement of the  $\text{MnO}_6$  octahedra has occurred and charges are strongly localized within distorted octahedra. It is finally worth to notice that, at present, it is quite difficult to determinate the cause/effect relationship between charge-localization and octahedral rotation since apparently they reinforce each other.

## 4 Conclusions

We have demonstrated the feasibility of accurate Raman measurements of very thin LSMO manganite films (down to 40 Å) and have shown how this technique can be a simple and powerful tool to monitor subtle structural modifications hardly detectable with conventional diffraction techniques in ultra-thin films ( $d < 100$  Å). The strong hardening of the bending and stretching phonons observed on decreasing  $d$  below 100 Å appears to be related to the  $d$ -dependence of  $T_P$ . This behaviour is compatible with a scenario where the film layers closest to the substrate interface consist of a lattice of distorted octahedra rotated from the equilibrium positions they take in the bulk. Further investigation is necessary to understand in detail the leading mechanism giving rise to the formation of these distorted layers, and how more information can be extracted from the Raman phonon spectrum.

## References

1. *Colossal Magneto-resistance Oxides*, edited by Y. Tokura, Monographs in Condensed Matter Science (Gordon and Breach, Reading, UK, 2000), and references therein
2. E. Dagotto, T. Hotta, A. Moreo, *Phys. Rep.* **344**, 1 (2001), and references therein
3. A.J. Millis, *Nature* **392**, 147 (1998)
4. A.M. Haghiri-Gosnet, J.P. Renard, *J. Phys. D: Appl. Phys.* **36**, R127 (2003), and references therein
5. J.S. Wang, Q. Li, *Appl. Phys. Lett.* **73**, 2360 (1999)
6. M. Bibes, S. Valencia, L. Balcells, J. Fontcuberta, M. Wojcik, E. Jedryka, S. Naldoski, *Phys. Rev. Lett.* **87**, 67210 (2001)
7. A.J. Millis, T. Darling, A. Migliori, *J. Appl. Phys.* **83**, 1588 (1998)
8. C.A. Perroni, V. Cataudella, G. De Filippis, G. Iadonisi, V. Marigliano Ramaglia, F. Ventriglia, *Phys. Rev. B* **68**, 224424 (2003)
9. R. Zhang, R.F. Willis, *Phys. Rev. Lett.* **86**, 2665 (2001)
10. A. de Andres, J. Rubio, G. Castro, S. Taboada, J.L. Martinez, J.M. Colino, *Appl. Phys. Lett.* **83**, 713 (2003)
11. J.Z. Sun, D.W. Abraham, R.A. Rao, C.B. Eom, *Appl. Phys. Lett.* **74**, 3017 (1999)
12. M. Bibes, S. Valencia, L. Balcells, B. Martinez, J. Fontcuberta, M. Wojcik, S. Naldoski, E. Jedryka, *Phys. Rev. B* **66**, 134416 (2002)
13. M.N. Iliev, M.V. Abrashev, V.N. Popov, V.G. Hadjiev, *Phys. Rev. B* **67**, 212301 (2003), and references therein
14. M. Angeloni, G. Balestrino, N. Boggio, P.G. Medaglia, P. Orgiani, A. Tebano, *J. Appl. Phys.* **96**, 6387 (2004)

15. M.N. Iliev, M.V. Abrashev, J. Raman Spectroscopy **32**, 805 (2001)
16. M.N. Iliev, M.V. Abrashev, H.G. Lee, V.N. Popov, Y.Y. Sun, C. Thomsen, R.L. Meng, C. W. Chu, Phys. Rev. B. **57**, 2872 (1998)
17. B. Podobedov, A. Weber, D.B. Romero, J.P. Rice, H.D. Drew, Phys. Rev. B **58**, 43 (1998)
18. M.V. Abrashev, A.P. Litvinchuk, M.N. Iliev, R.L. Meng, V.N. Popov, V.G. Ivanov, R.A. Chakalov, C. Thomsen, Phys. Rev. B **59**, 4146 (1999)
19. A. Congeduti, P. Postorino, E. Caramagno, M. Nardone, A. Kumar, D.D. Sarma, Phys. Rev. Lett. **86**, 1251 (2001)
20. V.B. Podobedov, A. Weber, D.B. Romero, J.P. Rice, H.D. Drew, Solid State Commun. **105**, 589 (1998)
21. S. Yoon, H.L. Liu, G. Schollerer, S.L. Cooper, P.D. Han, D.A. Payne, S.W. Cheong, Z. Fisk, Phys. Rev. B **58**, 2795 (1988)
22. N.M. Souza-Neta, A.Y. Ramos, H.C.N. Tolentino, E. Favre-Nicolin, L. Ranno, Appl. Phys. Lett. **83**, 3587 (2003)